

RESEARCH

Open Access



# Extracellular vesicle-bound S100A8/A9 is differentially expressed in septic shock and prompts acute lung injury

Jiangmei Wang<sup>1†</sup>, Weiliang Wu<sup>1†</sup>, Tingting Wen<sup>2</sup>, Guoping Zheng<sup>3</sup>, Guanguan Qiu<sup>3</sup>, Huifeng Qian<sup>3</sup>, Ruoyang Zhang<sup>1</sup>, Jie Xia<sup>1</sup>, Yaoqin Hu<sup>1</sup>, Ruoqiong Huang<sup>1</sup>, Ruoxi Zang<sup>1</sup>, Zhenkai Le<sup>1</sup>, Qiang Shu<sup>1,4\*</sup> and Jianguo Xu<sup>1,4\*</sup>

## Abstract

**Background** Sepsis is a common indirect insult leading to acute respiratory distress syndrome (ARDS). Circulating extracellular vesicles (EVs) have been reported to participate in the pathogenesis of sepsis. However, the alteration of EV-bound S100A8/A9 during septic shock, along with the role of S100A8/A9 in driving acute lung injury, remains unexplored.

**Methods** EVs were isolated from the plasma of patients upon admission with sepsis or septic shock, as well as from healthy controls. Levels of EV S100A8/A9 were assayed via ELISA. To examine the effects and underlying mechanisms of septic shock EVs in acute lung injury, these EVs were administered intratracheally into wild-type C57BL/6 mice or mice with a deficiency of advanced glycation end-products (RAGE). In addition, a mouse model of polymicrobial sepsis was introduced using cecal ligation and puncture (CLP).

**Results** Levels of EV S100A8/A9 were significantly elevated in patients with sepsis or septic shock compared to healthy controls. Receiver operating characteristic (ROC) analysis demonstrated that EV S100A8/A9 effectively distinguished between septic shock and sepsis and had predictive potential for the development of ARDS. Notably, the levels of S100A8/A9 in EVs and alveolar macrophages from CLP mice were significantly higher than those in sham mice. Intratracheal administration of septic shock EVs directly induced acute lung injury and M1 macrophage polarization in a lipopolysaccharide-independent manner. Septic shock EVs were efficiently taken up by alveolar macrophages in vivo, leading to a significant increase in S100A8/A9 levels, which was inhibited by preincubating the EVs with an S100A8/A9 neutralizing antibody. Additionally, mice with deficiency in RAGE, a receptor for S100A8/A9, were partially protected from acute lung injury induced by septic shock EVs. In vitro, septic shock EVs prompted a proinflammatory response in bone marrow-derived macrophages. This response was blocked by preincubating the EVs with the S100A8/A9 neutralizing antibody.

<sup>†</sup>Jiangmei Wang and Weiliang Wu have contributed equally to this work.

\*Correspondence:

Qiang Shu  
shuqiang@zju.edu.cn  
Jianguo Xu  
jxu5@yahoo.com

Full list of author information is available at the end of the article



**Conclusions** Our results suggested that EV S100A8/A9 has potential value in distinguishing septic shock from sepsis and predicting the development of ARDS. Septic shock EVs-induced lung injury is at least partially mediated through S100A8/A9-RAGE pathway, involving the activation of alveolar macrophages.

**Keywords** Sepsis, Extracellular vesicles, Acute respiratory distress syndrome, Acute lung injury, S100A8/A9

## Background

Acute respiratory distress syndrome (ARDS, acute lung injury) is characterized by the acute onset of refractory dyspnea which is accompanied by bilateral infiltrates on chest radiograph that cannot be ascribed to heart failure. Despite supportive strategies such as neuromuscular blockage and lung protective ventilation, the mortality of ARDS still remains around 30–40% [1]. During early phase of lung injury, alveolar macrophages are activated by pathogens through pattern recognition receptors. Proinflammatory cytokines are released and stimulate the release of chemokines from neighboring alveolar epithelial cells and tissue macrophages, resulting in the recruitment of neutrophils and macrophages. The severe inflammatory responses lead to impaired barrier function of the alveolar epithelium and fluid accumulation in the air space [2].

One of the major underlying causes of ARDS is sepsis [3]. Sepsis is a lethal syndrome characterized by organ dysfunction as a result of dysregulated response to infection [4]. It is estimated that about 49 million patients worldwide were afflicted with sepsis in 2017, accounting for approximately 11 million sepsis-related deaths and almost one-fifth of yearly all global deaths [5]. At present, there is no specific treatment for sepsis-induced ARDS. There is a pressing need for deciphering the precise mechanisms of sepsis-induced ARDS.

Extracellular vesicles (EVs) are particles naturally secreted from cells [6]. Chargaff and West first documented the presence of EVs in 1946 as “minute breakdown products of blood corpuscles” [7]. The first electron microscopy image of EVs was documented in 1967 [8]. EVs, originally thought as a feature of waste removal for cells [9], now represent a unique means for intercellular communication [10, 11]. They have the capacity of mimicking the function of the parental cells and transferring functional miRNA/mRNA and protein cargos to target cells [12]. Our group reported that miR-27a-3p was transported from EVs of mesenchymal stem cells to alveolar macrophages and abated lung injury [13].

Intravenous injection of EVs from peripheral blood of septic patients significantly elevated the expression of proinflammatory proteins such as nuclear factor- $\kappa$ B (NF- $\kappa$ B) in the lungs and heart of mice [14]. Li et al. reported that sepsis EVs enhanced proinflammatory responses and apoptosis of cells related to lung tissue via delivery of

miR-210-3p [15]. Xu et al. reported that circulating EVs from septic mice prompted the production of proinflammatory cytokines in vitro via miRNA and TLR7-mediated signaling. The EVs also induced the recruitment of peritoneal leukocytes in vivo [16].

It has been documented that S100A8 and S100A9 exist as a heterodimer complex and are abundantly expressed in neutrophils, macrophages, and endothelial cells, representing up to 40% of neutrophil cytosolic proteins [17, 18]. The S100A8/A9 complex is a ligand for Toll-like receptor 4 (TLR4) and receptor for advanced glycation endproducts (RAGE), promoting proinflammatory responses [19]. Plasma S100A8/A9 has been reported as a disease marker for sepsis and a predictor for outcomes [20]. The first aim of this study was to examine whether there is an alteration of EV S100A8/A9 in sepsis and septic shock patients. The second aim was to determine whether EV S100A8/A9 contributes to septic shock-induced lung injury.

## Materials and methods

### Study subjects

Sepsis and septic shock patients were consecutively enrolled into the prospective observational study conducted at the ICU of the First Affiliated Hospital of Zhejiang University School of Medicine between September 2022 and May 2024. All enrolled patients met the consensus Sepsis-3 classification [4]. Eligible patients were at least 18 years old and diagnosed with sepsis during the first 24 h after admission. Subjects were excluded from the study if any of the following criteria were met: age less than 18, pregnancy, undergoing immunosuppressive or chemotherapy, chronic inflammatory diseases, current COVID-19/HBV/HCV/HIV infection, and traumatic brain injury. Healthy control subjects were age-matched volunteers without concurrent infection and enrolled during physical examination. After the inclusion, all participants or legal representatives were provided with written details of the study. The study was only conducted in participants with written informed consent. Study procedures were in obedience to the provisions detailed in Declaration of Helsinki. The study protocol was approved by the ethics committee of the First Affiliated Hospital of Zhejiang University School of Medicine. For enrolled subjects, whole peripheral blood was collected up to 24 h after ICU admission. In the healthy

controls, whole peripheral blood was collected immediately after written informed consent. Demographic characteristics, causes of infection, microbiology results, sequential organ failure assessment (SOFA) scores, acute physiology and chronic health evaluation II (APACHE II) scores, laboratory measurements, development of ARDS, lengths of hospital stay, and ICU mortality were collected from the medical record for study purpose.

#### Isolation and labeling of EVs from plasma

Peripheral blood samples were collected in EDTA tubes and centrifuged at 800 g for 10 min within 4 h of sample collection. After centrifugation, plasma samples were carefully collected and stored in a  $-80^{\circ}\text{C}$  freezer until use. Plasma samples were thawed and placed into SW 32 Ti centrifuge tubes (Beckman Coulter, Brea, CA), diluted with phosphate buffered saline (PBS) to the appropriate height, and centrifuged at 10,000 g for 30 min. Then, the top fraction was poured into a new SW 32 Ti centrifuge tube and centrifuged at 120,000 g for 120 min. The pellet of the centrifugation was washed with 9 ml of PBS, transferred to a SW 41 Ti centrifuge tube, and centrifuged at a second 120,000 g for 120 min. The EV-containing pellet was resuspended

with 50  $\mu\text{l}$  PBS. The EV yield was determined by measuring the protein content using the Pierce BCA protein detection kit (Thermo Fisher, Waltham, MA) (A list of commercial reagents is provided in Supplemental Table 1). For assay of EV cargo transfer in vivo, labeling of EVs with Vybrant™ DiD (Thermo Fisher) was performed as described previously [13].

For visualization of transferred EV cargo in pulmonary macrophages in vivo, septic shock EVs were labeled with fluorescent dye Vybrant DiD and instilled to mice intratracheally. After 24 h, lung tissue samples were harvested and embedded in Tissue-Tek OCT (Sakura), sectioned to a thickness of 5  $\mu\text{m}$ , fixed with 4% formaldehyde for 1 h, dehydrated with 30% sucrose for 24 h, and permeabilized with 0.3% Triton X-100 for 30 min. Sections were then blocked with blocking solution containing 0.5% Tween 20 and 5% bovine serum albumin for 1 h and incubated with a rabbit anti-F4/80 antibody (Abcam) overnight. After that, the sections were incubated with CoraLite 488-conjugated goat anti-rabbit IgG (Proteintech, Wuhan, China) for 1 h. Cell nuclei were labeled with 1  $\mu\text{g}/\text{ml}$  DAPI, and images were taken with a Zeiss fluorescence microscope.

**Table 1** Demographic and clinical characteristics of sepsis and septic shock patients

Variable	Sepsis n = 28	Septic shock n = 26	Healthy controls n = 24	<i>p</i> value
Age (years) $\pm$ SD	62.5 $\pm$ 19.4	67.0 $\pm$ 14.6	62.8 $\pm$ 8.3	> 0.05
Male/female (n)	21/7	17/9	17/7	> 0.05
Type of organism, n (%)			N/A	> 0.05
Gram +	2 (7.1)	2 (7.7)		
Gram –	15 (53.6)	12 (46.1)		
Fungus	4 (14.3)	2 (7.7)		
Compound	1 (3.6)	7 (26.9)		
No organism cultured	6 (21.4)	3 (11.5)		
Source of infection, n (%)			N/A	> 0.05
Pneumonia	19 (67.9)	12 (46.1)		
Peritonitis	6 (21.4)	4 (15.4)		
Urinary infection	1 (3.6)	3 (11.5)		
Other	2 (7.1)	7 (26.9)		
SOFA score $\pm$ SD	6.64 $\pm$ 2.30	11.19 $\pm$ 5.28	N/A	< 0.001
APACHE II score $\pm$ SD	18.75 $\pm$ 6.14	23.31 $\pm$ 9.27	N/A	< 0.05
CRP (mg/L) $\pm$ SD	90.72 $\pm$ 78.20	146.70 $\pm$ 95.04	N/A	< 0.05
PCT (ng/ml) $\pm$ SD	3.02 $\pm$ 4.54	22.39 $\pm$ 31.74	N/A	< 0.05
Lactic acid (mmol/L) $\pm$ SD	1.49 $\pm$ 0.82	3.14 $\pm$ 2.64	N/A	< 0.01
ARDS, n (%)	8 (28.5)	16 (61.5)	N/A	< 0.01
ICU length of stay, day (IQR)	7.5 (5, 20.25)	20 (10, 31.25)	N/A	< 0.05
ICU 28 day Death, n (%)	3 (10.7)	12 (46.1)	N/A	< 0.01

SD standard deviation, IQR inter quartile range, N/A not applicable, SOFA sequential organ failure assessment, APACHE acute physiology and chronic health evaluation, CRP C-reactive protein, PCT procalcitonin, ARDS acute respiratory distress syndrome, ICU intensive care unit

### Western blot analysis

Cells and EVs were treated with RIPA buffer (Applygen, China) supplemented with proteinase inhibitor cocktail for 30 min. BCA protein assay kit was used for determination of protein concentration of lysates. An equal amount of protein (10  $\mu$ g) was resolved on 12% SDS-PAGE gel and transferred to polyvinylidene difluoride membranes (Millipore, Billerica, MA). The membranes were incubated for 1 h with blocking buffer (PBS with 0.1% Tween-20 and 5% non-fat milk). Then, membranes were incubated with the primary antibodies for S100A8/A9 (Abcam, Cambridge, UK),  $\beta$ -actin (Cell Signaling Technology, Danvers, MA), and CD9 (Abcam) overnight at 4  $^{\circ}$ C, followed by corresponding secondary antibodies. The membranes were developed using EZ-ECL Detection Kit (BDBIO, Hangzhou, China).

### ELISA analysis

S100A8/A9 ELISA was performed following the manufacturer's instruction (Proteintech). The plates were incubated at 37  $^{\circ}$ C for 1 h with 200  $\mu$ L of blocking solution, followed by three washes with PBS with 1% Tween 20 (PBS-T buffer). EVs were lysed with extraction buffer PTR (Abcam). EVs (20  $\mu$ g/ml) and plasma (samples with uniform dilution factor) were incubated in each well for 1.5 h at 37  $^{\circ}$ C. The plates were washed 3 times with PBS-T buffer, then 50  $\mu$ L of horseradish peroxidase-conjugated substrate was added to each well. After a 30-min incubation at room temperature, the reactions were halted by the addition of 25  $\mu$ L of 1 N H<sub>2</sub>SO<sub>4</sub>. The optical density was examined at 450 nm using SpectraMax 190 Microplate Reader (Molecular Devices, San Jose, CA).

### Mouse model of EV-induced lung injury

RAGE<sup>-/-</sup> mice with C57BL/6 J background were generated by the Nanjing Biomedical Research Institute of Nanjing University via CRISPR/Cas9 technology and maintained in the lab. Wild-type (WT) C57BL/6 J mice (male, 6–8 weeks old) were acquired from Shanghai Laboratory Animal Center (Shanghai, China). The animal study protocol was approved by the Institutional Animal Care and Use Committee of Zhejiang University School of Medicine. The mice were housed under a 12-h light/dark cycle at a controlled temperature of 24  $\pm$  1  $^{\circ}$ C, with ad libitum access to food and water. Polymyxin B

(PMB, 25  $\mu$ g/ml) was incubated with septic shock EVs at 37  $^{\circ}$ C for 1 h to neutralize the possibly contaminated lipopolysaccharide (LPS) in EVs. Mice (male, 6–8 weeks old) were randomized into different groups and anesthetized by intraperitoneal administration of single dose of phenobarbital (50 mg/kg). Mice were instilled intratracheally with PBS (50  $\mu$ L), control EVs (100  $\mu$ g/50  $\mu$ L), septic shock EVs (100  $\mu$ g/50  $\mu$ L), and septic shock EVs (100  $\mu$ g/50  $\mu$ L) + PMB. Mice were sacrificed at 24 h after treatment. Specimens of lung as well as bronchioalveolar lavage (BAL) were collected for subsequent examination.

### Mouse model of polymicrobial sepsis

Animal model of experimental sepsis was generated in a BSL2 lab via cecal ligation and puncture (CLP) as previously described [21]. Mice were weighed and anesthetized by intraperitoneal administration of a single dose of phenobarbital (50 mg/kg). The cecum was exposed by a 2-cm midline laparotomy incision. A 3–0 silk suture was used to ligate the cecum at about one centimeter from cecal tip. The cecum was perforated twice with a 21-gauge needle at the distal point of the ligation. The cecum was gently pressured with 2 fingers to extrude fecal material at the puncture site and repositioned to the abdominal cavity. Two layers of 4–0 silk sutures were used to close the peritoneum. For mice in the sham group, the same procedure was conducted without ligation and puncture of the cecum. All mice received 1 ml of isotonic saline solution subcutaneously to provide hydration. Mice were sacrificed via cervical dislocation at 48 h after CLP or sham surgery to collect BAL and blood samples.

### Bone marrow-derived macrophages (BMDMs) and treatment

Femurs and tibias of sacrificed C57BL/6 mice were flushed with PBS using 25-gauge needles. Bone marrow was collected by centrifugation for 5 min at 300 g and resuspended in red blood cell lysis buffer for 5 min. Cells were spun down and resuspended in differentiation medium (DMEM supplemented with 20 ng/ml GM-CSF, 10% FBS). After overnight culture at 37  $^{\circ}$ C with 5% CO<sub>2</sub>, non-adherent cells were saved and cultured on 6-well plates. Cells were replenished with fresh differentiation medium every 3 days. On day 7, fully differentiated

(See figure on next page.)

**Fig. 1** EV S100A8/A9 levels and their correlation with plasma S100A8/A9 levels, disease severity scores, and sepsis biomarkers. The box and whisker plots depict the concentration of EV S100A8/A9 (A) and plasma S100A8/A9 (B) of healthy controls (n=24), sepsis patients (n=28), and septic shock patients (n=26). The plots display the median (line inside boxes), interquartile range (box boundaries), and error bars (upper and lower ranges) (A-B). \* p < 0.05 and \* \* \* p < 0.001. The correlation curve was plotted by EV S100A8/A9 levels at admission to their corresponding plasma S100A8/A9 levels (C), along with APACHE-II (D), SOFA (E), CRP (F) and PCT (G) values. ns: not significant

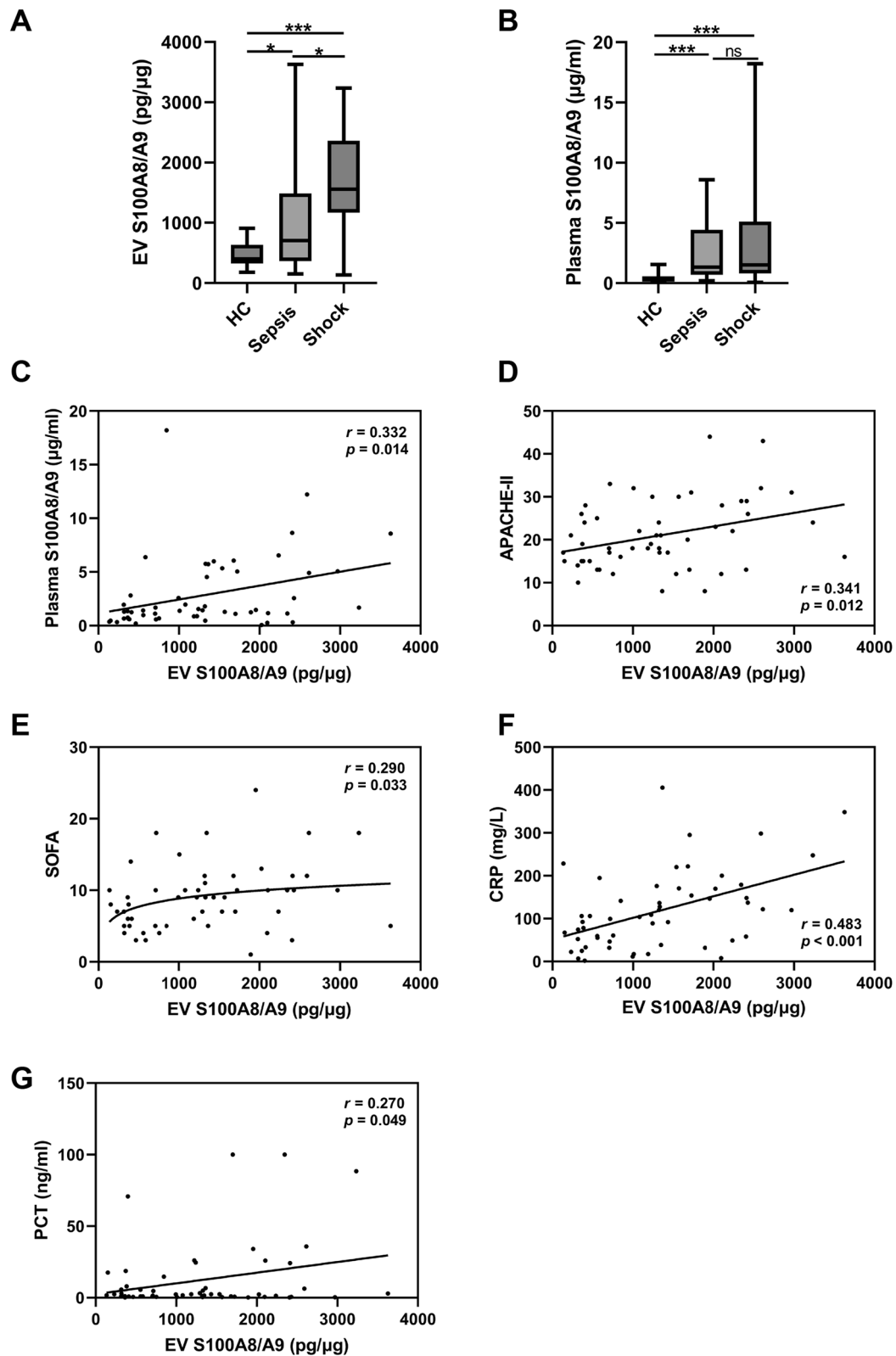


**Fig. 1** (See legend on previous page.)

macrophages were dissociated from the culture and replated at  $5 \times 10^5$  cells/well in 12-well plates. Polymyxin B (PMB, 25  $\mu\text{g/ml}$ ) was incubated with septic shock EVs at 37 °C for 1 h to neutralize the possibly contaminated LPS in EVs. Cells were treated with PBS, control EVs (100  $\mu\text{g/ml}$ ), septic shock EVs (100  $\mu\text{g/ml}$ ), and septic shock EVs+PMB for 24 h. Then, cells were collected for flow cytometry analysis. IL-1 $\beta$ , IL-6, TNF- $\alpha$ , and MIP-2 levels in the culture supernatants were assayed via ELISA (Multi Sciences, Hangzhou, China) per manufacturer's protocol. To examine the role of S100A8/A9 in the proinflammatory effects of septic shock EVs, the septic shock EVs were incubated overnight at 4 °C with or without an anti-S100A8/A9 neutralization antibody (Clone A15105B, BioLegend) at 100  $\mu\text{g/ml}$  prior to treatment of BMDMs. Cells were treated with PBS, control EVs (100  $\mu\text{g/ml}$ ), septic shock EVs (100  $\mu\text{g/ml}$ ), and septic shock EVs+anti-S100A8/A9 for 24 h. Culture supernatants were assayed for IL-6 and TNF- $\alpha$  via ELISA.

#### Protein leakage, neutrophil counts, and cytokine levels in bronchoalveolar (BAL)

BAL fluid was harvested from mice at 24 h after treatment of EVs. The BAL was pelleted via centrifugation at 500 g for 5 min. Protein concentration of the supernatant was examined using Pierce BCA Protein Assay Kit. Total white blood cells in the pellet were counted using a hemocytometer. Infiltrated neutrophils in the cell pellet were stained with a FITC-labeled anti-Ly-6G antibody (BD Biosciences) and examined by flow cytometry. BAL supernatant was also measured for IL-6 and TNF- $\alpha$  via ELISA.

#### Separation of primary alveolar macrophages from BAL

To isolate alveolar macrophages, BAL was processed immediately after collection and pelleted by centrifugation at 300 g for 5 min. Total cells were then resuspended with RPMI-1640 with 5% fetal bovine serum and plated onto 6-well plate ( $5 \times 10^5$  cells/well) in a 37 °C incubator with 5% CO<sub>2</sub>. After 1.5 h, the medium and non-adherent cells were discarded. The adhered macrophages were harvested with cold PBS for further experiments. The purity of the primary macrophages was consistently  $\geq 90\%$  for all samples (Supplemental Fig. 1).

#### Flow cytometry

To determine the polarization of macrophages in BAL and BMDMs, cells were resuspended in staining buffer (PBS, 0.5% BSA). Cells were incubated for 30 min with the anti-mouse antibodies or their isotype controls: PE-F4/80 and BV650-CD86 (BD Biosciences). For intracellular staining of iNOS and CD206, cells were treated with Fixation/Perm working buffer following the manufacturer's instructions (Foxp3/Transcription Factor Staining Buffer Set, Thermo Fisher) and incubated for 30 min with the anti-mouse antibodies or their isotype controls: BV785 CD206 (BioLegend, San Diego, CA) and PE-Cy7 iNOS (Thermo Fisher). Cells were washed twice with staining buffer and fixed with 4% paraformaldehyde. Flow cytometry data was collected on a BD LSRFortessa™ and analyzed using FlowJo V10 software.

#### Histopathology

Examination of lung histology was conducted on lungs without lavage. After euthanasia, an 18-gauge blunt needle was placed into the trachea and tightened using a ligature. After chest opening, the lungs were perfused gently with 4% buffered paraformaldehyde, removed, and fixed with the same solution for 24 h in a glass vial. The lungs were dehydrated in an automatic tissue processor and embedded in paraffin. Tissue sections of 5  $\mu\text{m}$  in thickness were deparaffinized using xylene, rehydrated with ethanol series, and processed with hematoxylin and eosin (H&E) staining before morphological structure evaluation. Images of lung sections were captured by a digital camera using an Olympus VS120 microscope (Shinjuku, Tokyo, Japan).

#### Statistical analysis

SPSS 27 software and GraphPad Prism 8.0.2 software were applied for statistical analysis. Categorical variables were displayed as percentages, and the significance of group differences was assessed using Pearson's chi-square test or Fisher's exact test. For quantitative data, normality was tested using the D'Agostino-Pearson Omnibus normality test, the Shapiro-Wilk normality test, and Kolmogorov-Smirnov test, with *p* value corrected by the Dallal-Wilkinson-Lilliefors method. Student *t* test or one-way/two-way analysis of variance with Bonferroni post

(See figure on next page.)

**Fig. 2** The value of EV S100A8/A9 for the prediction of septic shock and ARDS. **A** ROC curve displays sensitivity and specificity of EV and plasma S100A8/A9 in differentiating sepsis or septic shock from healthy controls. **B** ROC curve displays sensitivity and specificity of EV S100A8/A9, plasma S100A8/A9, CRP and PCT in predicting septic shock. **C** The box and whisker plots depict the concentration of EV S100A8/A9 and plasma S100A8/A9 in sepsis and septic shock patients who developed ARDS ( $n=24$ ) compared to those without ARDS ( $n=30$ ). The plots display the median (line inside boxes), interquartile range (box boundaries), and error bars (upper and lower ranges). **D** ROC curve displays sensitivity and specificity of EV S100A8/A9 and plasma S100A8/A9 in predicting ARDS. \* $p < 0.05$ . ns: not significant

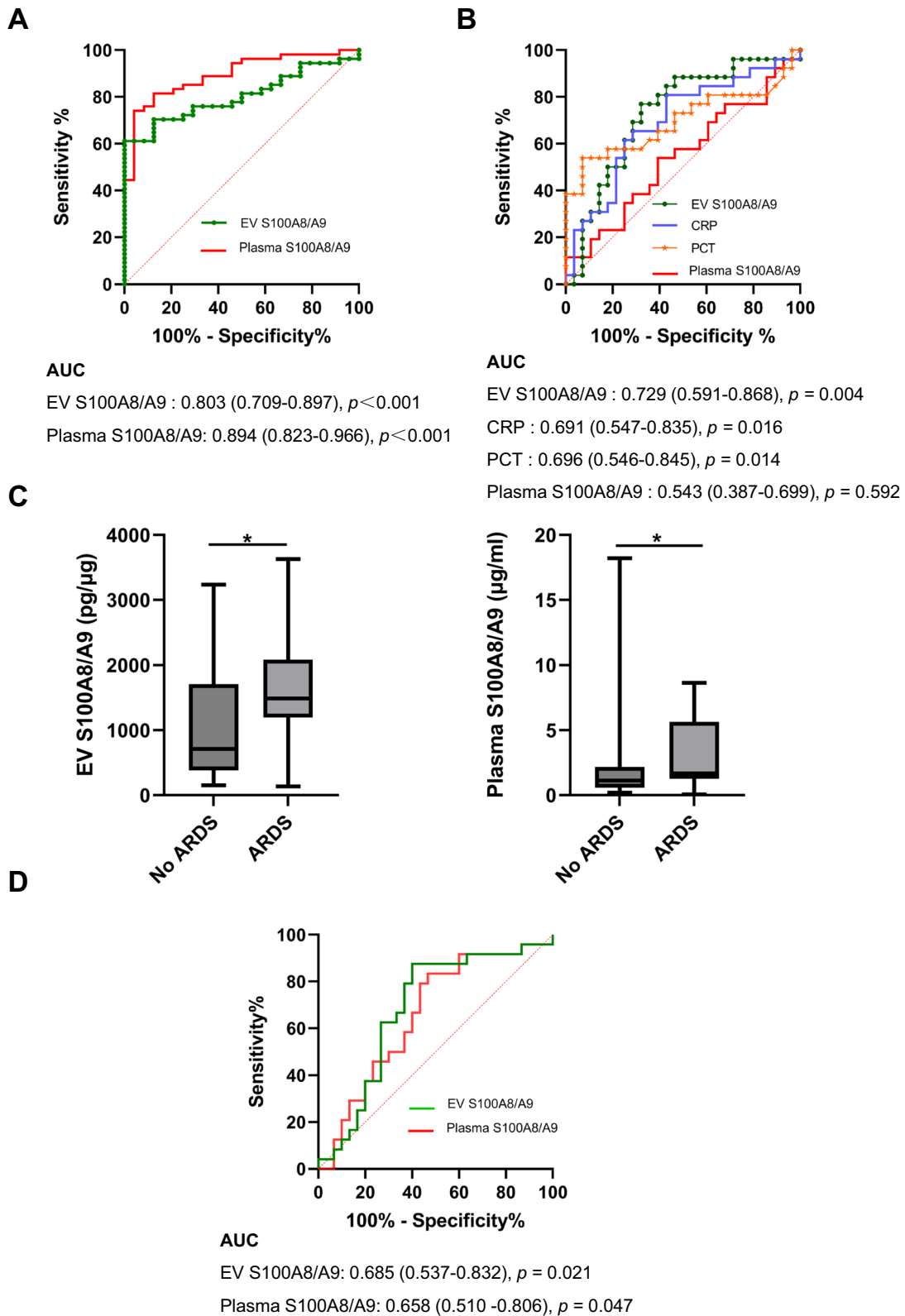


**Fig. 2** (See legend on previous page.)

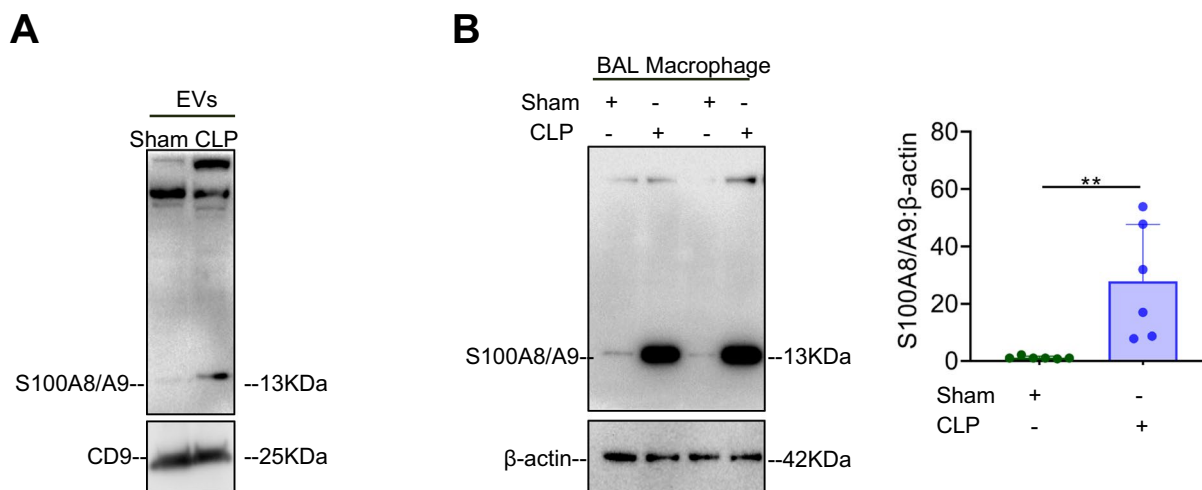


**Fig. 3** Expression of S100A8/A9 in CLP EVs and alveolar macrophages. **A** Samples of control and CLP EVs at 48 h after CLP procedure were resolved in SDS-PAGE gel and probed with an antibody for S100A8/A9. **B** BAL samples from control and CLP mice were collected at 48 h after procedure. Alveolar macrophages were separated and examined for the expression of S100A8/A9. Data are expressed as mean  $\pm$  SD,  $n = 6$  (**D**). **\*\*** $p < 0.01$

hoc analysis was performed for parametric data. Non-parametric data were examined using the Mann–Whitney test or the Kruskal–Wallis test with Dunn post hoc analysis. A  $p$  value of less than 0.05 was regarded as statistically significant.

## Results

### Study patient characteristics

Twenty-eight patients with clinical diagnosis of sepsis, 26 patients with septic shock, and 24 healthy controls were recruited for the study. The clinical characteristics, demographics data, and outcomes for patients were shown in Table 1. There was no statistically significant difference in age and gender among the three groups (all  $p > 0.05$ ). The source of infection and type of organisms responsible for the infection were similar between sepsis and septic shock. Septic shock patients had higher SOFA scores, APACHE II scores, c-reactive protein (CRP), procalcitonin (PCT), lactic acid, rate of ARDS, rate of mortality, and ICU/hospital lengths of stay.

### Plasma and EV S100A8/A9 are elevated in sepsis and septic shock patients

EVs from sepsis patients, septic shock patients, and healthy controls were separated by ultracentrifugation and characterized as our previous report [21]. The protein levels of S100A8/A9 in plasma and EVs at admission were examined via ELISA. EV (Fig. 1A) and plasma (Fig. 1B) S100A8/A9 were significantly higher in both sepsis and septic shock patients compared to healthy controls. Meanwhile, septic shock patients exhibited higher levels of EV S100A8/A9 (interquartile 1169 to 2360 pg/ $\mu$ g) compared to sepsis patients (interquartile 365–1486 pg/ $\mu$ g) (Fig. 1A), while there was no difference in plasma S100A8/A9 between septic shock (interquartile 0.772 to 4.626  $\mu$ g/ml) and sepsis (interquartile 0.690–4.423  $\mu$ g/ml) (Fig. 1B). EV S100A8/A9 from sepsis or septic shock patients was significantly correlated with plasma S100A8/A9 ( $p < 0.05$ , Fig. 1C), APACHE II score ( $p < 0.05$ , Fig. 1D), SOFA score ( $p < 0.05$ , Fig. 1E), CRP ( $p < 0.001$ , Fig. 1F), and PCT ( $p < 0.05$ , Fig. 1G).

(See figure on next page.)

**Fig. 4** LPS-independent effect of septic shock EVs on acute lung injury. Mice were randomized and treated with four regimens: PBS, control EVs (100  $\mu$ g/50  $\mu$ l), septic shock EVs (100  $\mu$ g/50  $\mu$ l), and septic shock EVs + PMB (25  $\mu$ g/ml pretreatment). PBS and EVs were administered intratracheally. Mice were sacrificed 24 h after treatment. **A** Microscopic images were obtained from lung sections stained with H&E. The arrows denote neutrophil infiltration. **B** BAL was examined for lung injury parameters, which included total protein content, total cell count, and neutrophil count. **C** BAL levels of IL-6 and TNF- $\alpha$  were examined via ELISA. Data are expressed as mean  $\pm$  SD,  $n = 8$ –9. \* $p < 0.05$ , \*\* $p < 0.01$ , \*\*\* $p < 0.001$

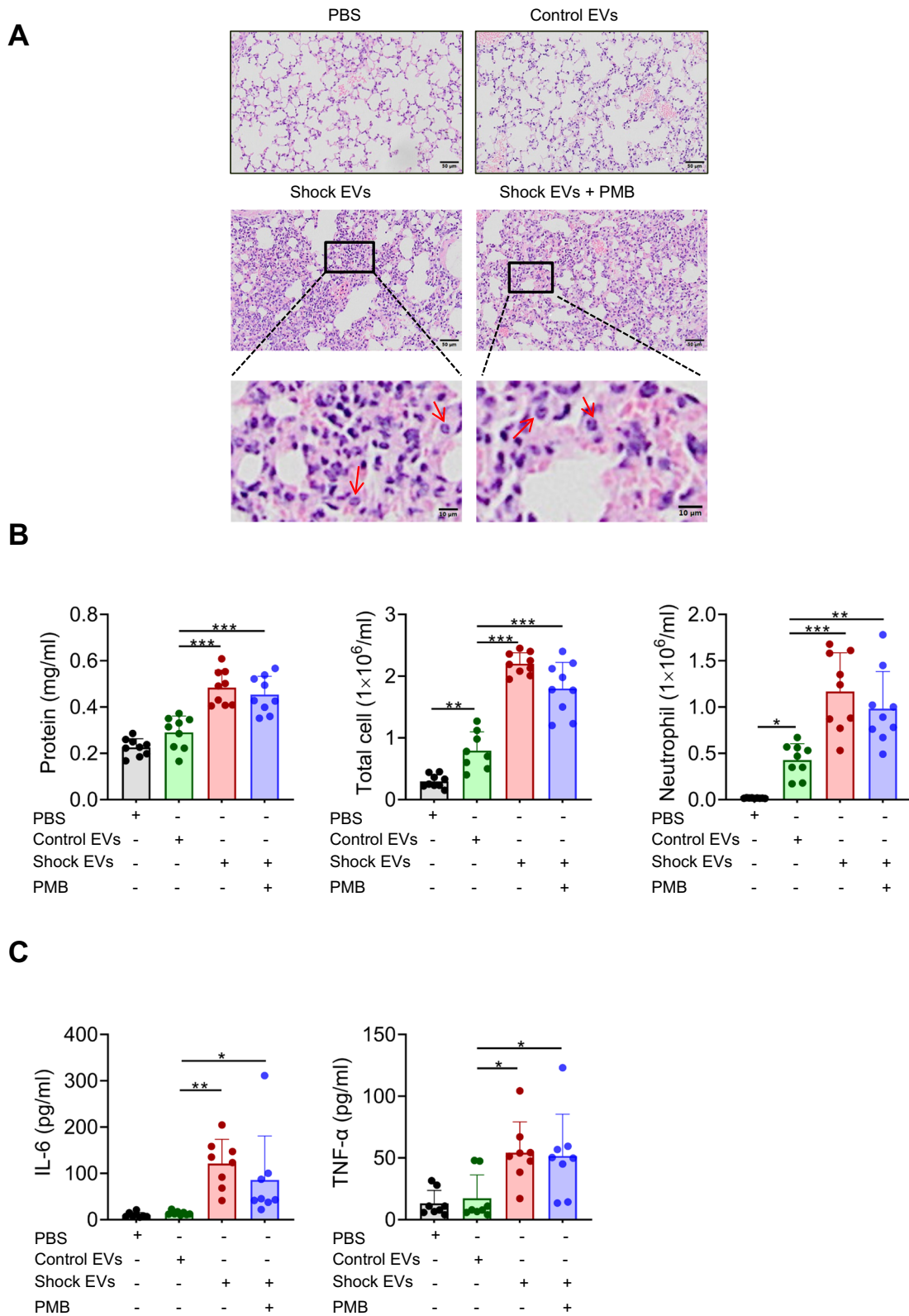


**Fig. 4** (See legend on previous page.)

### EV S100A8/A9 differentiates septic shock from sepsis and predicts the development of ARDS

The value of plasma and EV S100A8/A9 in discriminating between patients with sepsis or septic shock and healthy controls was determined by receiver operating characteristic (ROC) analysis. EV S100A8/A9 had an area under the curve (AUC) of 0.803 (95% CI 0.709–0.897,  $p < 0.001$ ), while the AUC for plasma S100A8/A9 was 0.894 (95% CI 0.823–0.966,  $p < 0.001$ ) (Fig. 2A). Nevertheless, there was no significant difference in the AUC between EV S100A8/A9 and plasma S100A8/A9 ( $p = 0.096$ ). ROC curve analysis was also conducted to evaluate the value of plasma and EV S100A8/A9, along with plasma CRP and PCT, in differentiating sepsis and septic shock. The AUC for EV S100A8/A9 (AUC = 0.729; 95% CI 0.591–0.868;  $p = 0.004$ ) was comparable to that of CRP (AUC = 0.691; 95% CI 0.547–0.835;  $p = 0.016$ ) and PCT (AUC = 0.696; 95% CI 0.546–0.845;  $p = 0.014$ ) (Fig. 2B), indicating their predictive value for septic shock. However, plasma S100A8/A9 (AUC = 0.543; 95% CI 0.387–0.699;  $p = 0.592$ ) did not show predictive value for septic shock.

The levels of EV and plasma S100A8/A9 were significantly elevated in sepsis and septic shock patients who developed ARDS compared to those without ARDS (Fig. 2C). The predictive value of plasma and EV S100A8/A9 for the development of ARDS was determined by ROC analysis. EV S100A8/A9 exhibited an AUC of 0.685 (95% CI 0.537–0.832,  $p = 0.021$ ), while the AUC for plasma S100A8/A9 was 0.658 (95% CI 0.510–0.806,  $p = 0.047$ ) (Fig. 2D). While serum S100A8/A9 has previously been identified as a potential biomarker for predicting ARDS onset [22], these findings suggest that EV S100A8/A9 may serve as a promising biomarker for early prediction of ARDS.

### EV S100A8/A9 is elevated in CLP mice

In Western blot analysis, plasma EVs from the CLP mice had high levels of S100A8/A9 while expression in the sham group was mostly undetectable (Fig. 3A). Furthermore, alveolar macrophages from CLP mice had much

higher levels of S100A8/A9 compared with those from sham mice (Fig. 3B). Previous studies have documented the proinflammatory nature of S100A8/A9 [23]. These findings from the animal model suggest the involvement of EV S100A8/A9 in sepsis-associated inflammation.

### Septic shock EVs directly prompt acute lung injury in mice

To determine whether septic shock EVs could evoke lung injury, C57BL/6 mice were exposed to intratracheal delivery of septic shock or control EVs (100  $\mu\text{g}$ /mouse in 50  $\mu\text{l}$ ). BAL and lung specimen were collected at 24 h after insult. H&E staining results showed that septic shock EVs elicited neutrophil infiltration in the lung, which was accompanied by thickened alveolar septum and augmented interstitial cellularity compared with control EVs (Fig. 4A). PMB treatment of septic shock EVs did not mitigate the histological alterations, indicating that LPS was not a contributing factor for the effect of septic shock EVs (Fig. 4A). Enhanced alveolar-capillary barrier permeability (BAL protein level) is a hallmark of acute lung injury. BAL protein levels, total cell number, and neutrophil number were significantly elevated (by 66%, 178%, and 173%, respectively) after treatment with septic shock EVs versus control EVs (Fig. 4B). Although control EVs had no effect on the BAL protein levels, it is noteworthy that they caused a modest increase in total cells and neutrophils as compared with PBS. PMB treatment of septic shock EVs did not alter the parameters for lung injury (Fig. 4B). Levels of BAL IL-6 and TNF- $\alpha$  were significantly increased (by 7.6-fold and 2.2-fold, respectively) in septic shock group versus control group (Fig. 4C). In the meantime, PMB treatment did not alter the effect of septic shock EVs on BAL IL-6 and TNF- $\alpha$  levels.

### Septic shock EVs promote M1 macrophage polarization in vivo

BAL samples as described above were examined for macrophage phenotypes via flow cytometry (Fig. 5A). Septic shock EVs significantly increased the populations of F4/80 + iNOS + cells as well as F4/80 + CD86 + cells compared with control EVs, favoring polarization of alveolar

(See figure on next page.)

**Fig. 5** Alveolar macrophage polarization in vivo after insult of septic shock EVs. Mice were randomized and treated with four regimens: PBS, control EVs (100  $\mu\text{g}$ /50  $\mu\text{l}$ ), septic shock EVs (100  $\mu\text{g}$ /50  $\mu\text{l}$ ), and septic shock EVs + PMB (25  $\mu\text{g}$ /ml pretreatment). BAL fluid cells were collected at 24 h and stained with a combination of PE anti-F4/80, BV650 anti-CD86, BV785 anti-CD206, and PE-Cy7 anti-iNOS or with the isotype control for 30 min. **A** Dot plots displayed the gating strategy to identify polarization of alveolar macrophages. **B** Representative dot plot showed F4/80 + iNOS + and F4/80 + CD86 + (M1) macrophages in flow cytometry. **C** Representative dot plot displayed F4/80 + CD206 + (M2) macrophages. Numbers in the plot denote the percentage of cells in the gate for that particular experiment. Data for macrophage polarization were plotted in the right panels. Data are expressed as mean  $\pm$  SD,  $n = 8$ –9. \* $p < 0.05$ , \*\* $p < 0.01$ , \*\*\* $p < 0.001$

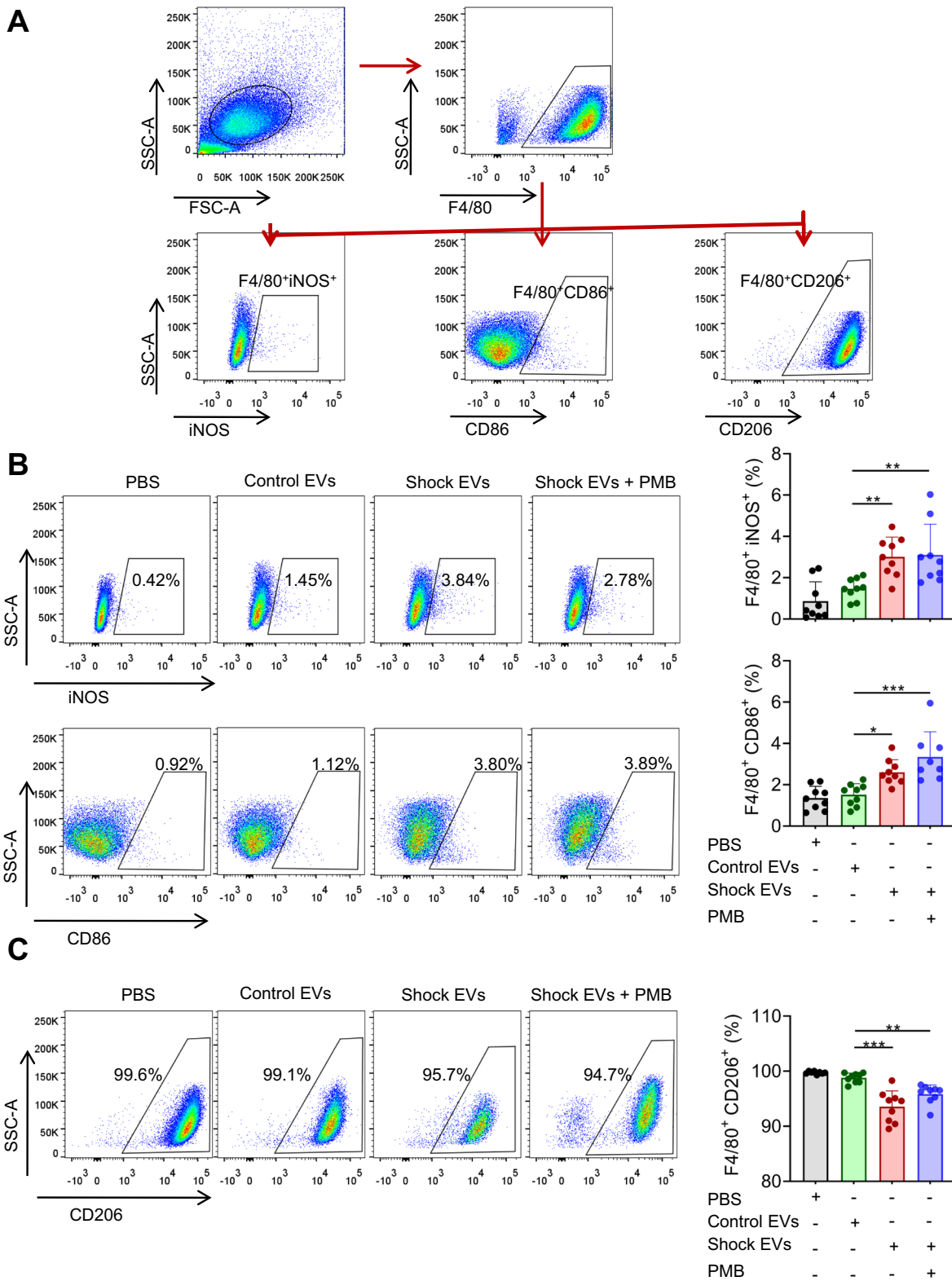


**Fig. 5** (See legend on previous page.)

macrophages toward M1 phenotype (Fig. 5B). Additionally, septic shock EVs reduced the expression of markers for M2 macrophages (F4/80+CD206+) (Fig. 5C). Pretreatment of septic shock EVs with PMB did not alter the effect of EVs on macrophage phenotypes (Fig. 5B, C).

### Septic shock EVs enhance inflammatory response in vitro via S100A8/A9

To examine whether septic shock EVs modulate macrophage polarization in vitro, BMDMs were allocated into 4 groups: PBS, control EVs, septic shock EVs, and septic shock EVs with PMB pretreatment. After 24 h of treatment, cells were analyzed for macrophage phenotypes via flow cytometry (gating strategy in Supplemental Fig. 2). Phenotype results revealed that septic shock EVs elevated the expression of F4/80+iNOS+M1 macrophages compared with the control EVs (Fig. 6A), while the levels of F4/80+CD206+M2 macrophages were significantly reduced (Fig. 6B). Again, PMB treatment did not influence septic shock EV-induced macrophage polarization (Fig. 6A, B).

To examine whether septic shock EVs alter inflammatory response in vitro, expression of IL-1 $\beta$ , IL-6, MIP-2, and TNF- $\alpha$  in the culture medium was examined at 24 h via ELISA. Results showed that septic shock EVs significantly increased the levels of MIP-2, IL-1 $\beta$ , IL-6, and TNF- $\alpha$  compared to control EVs (Fig. 6C). As expected, the levels of proinflammatory cytokines were not affected by pretreatment of septic shock EVs with PMB. Interestingly, the proinflammatory effect of septic EVs on BMDMs was blocked by an anti-S100A8/A9 neutralization antibody (Clone A15105B) (Fig. 6D), suggesting that EV S100A8/A9 plays a significant role in mediating this inflammatory response.

### S100A8/A9 is transferred from septic EVs to alveolar macrophages

To study the efficiency of EV uptake by alveolar macrophages, septic shock EVs were labeled with fluorescent dye Vybrant DiD and instilled to mice intratracheally. At 24 h post-instillation, approximately 70% of BAL

macrophages were positive for EVs, indicating efficient transfer of EV cargo to alveolar macrophages in vivo (Fig. 7A). Confocal microscopy of lung sections further revealed that the Vybrant DiD-labeled septic shock EVs largely co-localized with the F4/80-expressing macrophages (Fig. 7B). The levels of S100A8/A9 in alveolar macrophages were significantly augmented 24 h after intratracheally administration of septic shock EVs compared to control EVs (Fig. 7C). Additionally, pre-incubation of septic shock EVs with an S100A8/A9 neutralizing antibody (100  $\mu$ g/ml) resulted in a significant reduction in S100A8/A9 levels in alveolar macrophages 24 h after administration of EVs (Fig. 7D). These findings suggest that S100A8/A9 may play an important role in facilitating the transfer of septic shock EVs to alveolar macrophages.

### RAGE deficiency alleviates septic shock EV-induced acute lung injury

Literature has documented that exogenous S100A8/A9 is proinflammatory and induces neutrophil influx to the lung in mice [23]. RAGE is a receptor for S100A8/A9 and is regarded as a biomarker for acute lung injury [24]. To explore the involvement of S100A8/A9-RAGE pathway in septic shock EV-evoked acute lung injury, WT and RAGE<sup>-/-</sup> mice were exposed to intratracheal administration of septic shock or control EVs (100  $\mu$ g/50  $\mu$ l). At 24 h after insult, BAL specimens were obtained for further analysis. Total protein levels, total cell counts, and neutrophil counts were significantly reduced (by 27.5%, 38.2%, and 36.4%, respectively) in RAGE<sup>-/-</sup> versus wild-type animals (Fig. 8A). Furthermore, RAGE deficiency diminished the effect of septic shock EVs on BAL IL-6 and TNF- $\alpha$  levels (Fig. 8B). These findings indicate that the acute lung injury induced by septic shock-derived EVs is at least partially mediated by S100A8/A9-RAGE pathway.

### Discussion

This report demonstrates that EV S100A8/A9 exhibits differential expression in septic shock patients versus those with sepsis and holds predictive potential for the onset of ARDS. In addition, the lung injury

(See figure on next page.)

**Fig. 6** Role of S100A8/A9 in septic shock EVs-induced proinflammatory response in vitro. **A–C** Mouse BMDMs were treated with four regimens: PBS, control EVs (100  $\mu$ g/ml), septic shock EVs (100  $\mu$ g/ml), or septic shock EVs + PMB (25  $\mu$ g/ml pretreatment). After 24 h, cells were collected and stained with a combination of PE anti-F4/80, BV785 anti-CD206, and PE-Cy7 anti-iNOS or with the isotype control for 30 min. **A** Representative dot plot showed iNOS+F4/80+ (M1) macrophages in flow cytometry. **B** Representative dot plot displayed CD206+F4/80+ (M2) macrophages. **A, B** Numbers in the plot denote the percentage of cells in the gate for that particular experiment. Data for macrophage polarization were plotted in the right panels. **C** Cell culture medium was collected at 24 h. Levels of IL-1 $\beta$ , IL-6, TNF- $\alpha$ , and MIP-2 in culture supernatants were examined by ELISA. **D** Septic shock EVs were preincubated with or without an anti-S100A8/A9 neutralization antibody before being applied to BMDMs as described above. Levels of IL-6 and TNF- $\alpha$  in culture supernatants were examined by ELISA. Data are expressed as mean  $\pm$  SD, n=6–9. \*p < 0.05, \*\*p < 0.01, \*\*\*p < 0.001

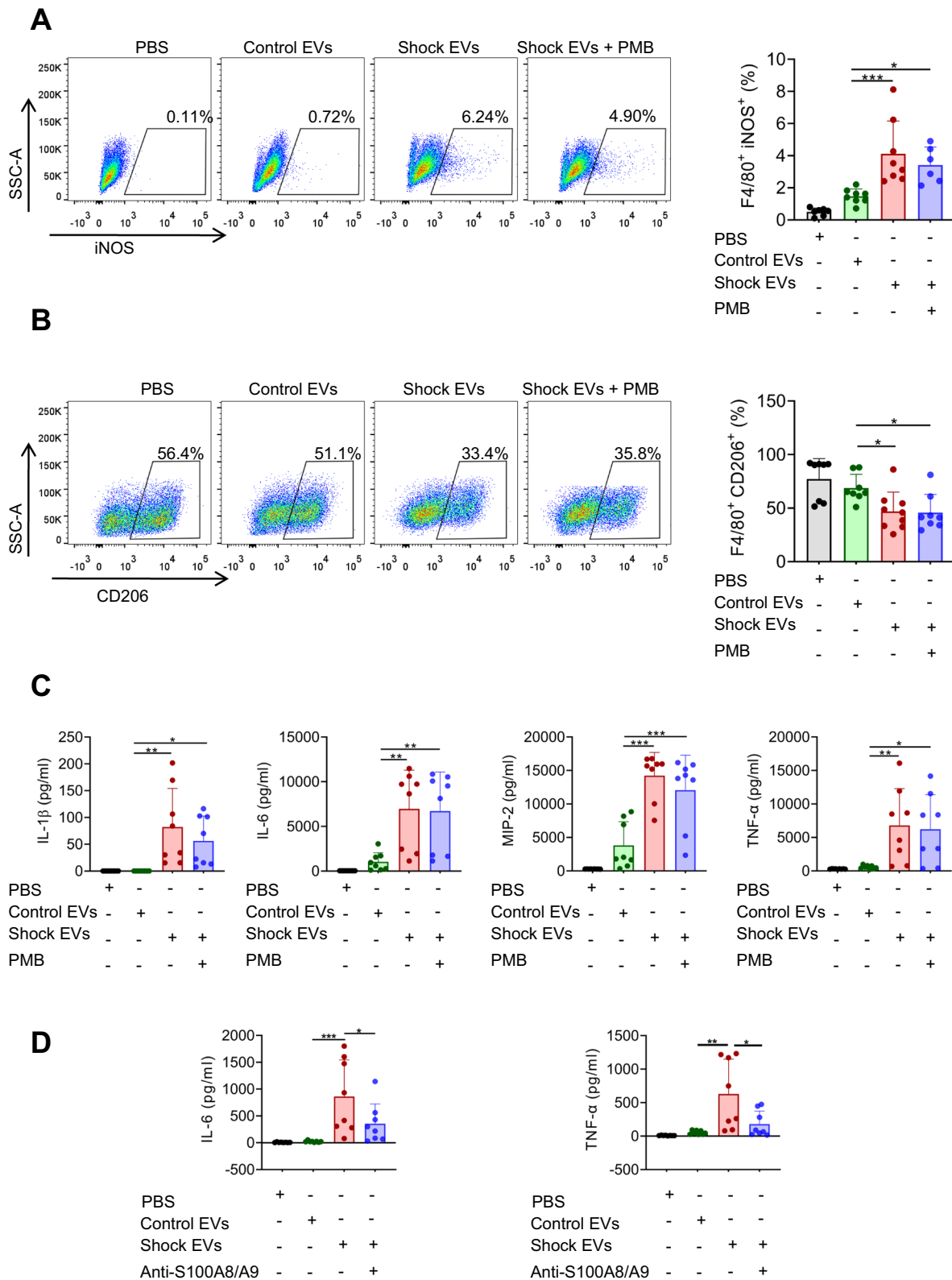


**Fig. 6** (See legend on previous page.)

induced by septic shock EVs is partly driven by the S100A8/A9-RAGE signaling pathway. Sepsis EVs have been reported to produce detrimental effects in other systems of the body. Platelet-derived EVs from septic shock patients depressed contractility of the left ventricle in isolated animal hearts. The negative inotropic effect was dependent on the nitric oxide in EVs [25]. When healthy rats were administered systemically with plasma EVs from septic rats, a septic inflammatory pattern was generated with upregulated NF- $\kappa$ B activity and oxidative stress [26]. In a rat model of CLP-induced sepsis, levels of procoagulant EVs were significantly increased and induced negative hemodynamic outcomes. Treatment of septic rats with activated protein C modified the levels of EVs, favoring hemodynamic improvement [27]. In addition, treatment of mice with GW4869, an EV release inhibitor, alleviated the CLP-induced cardiac inflammation, reduced pro-inflammatory cytokines, and prolonged survival [28]. Our findings address a knowledge gap regarding the role of sepsis EVs in the pathogenesis of ARDS.

Recent studies have highlighted the origins and mechanisms of S100A8/A9 in the development of sepsis and the progression of sepsis-related organ damage. Using scRNA-seq analysis, Wang et al. showed that S100A8/A9<sup>hi</sup> neutrophils accumulated in the lung tissues of septic mice, resulting in endothelial barrier damage and lung injury. These neutrophils induced mitochondrial dysfunction in endothelial cells, characterized by excessive fission and impaired mitophagy, via NDUFA3 suppression in mitochondrial complex I. Ultimately, mitochondrial DNA released from damaged mitochondria triggered ZBP1-mediated PANoptosis [29]. Jakobsson et al. demonstrated that myocardial dysfunction was associated with elevated S100A8/A9 levels in severe sepsis patients and CLP mice. Inhibition of the interaction between S100A8/A9 and RAGE using ABR-238901 effectively diminished systemic inflammation and restored the function of cardiac mitochondria [30]. Su et al. discovered that high levels of S100A8/A9 activated TLR4,

leading to platelet pyroptosis and a feedback loop that released inflammatory cytokines and stimulated neutrophil extracellular trap (NET) formation. Inhibiting the S100A8/A9-TLR4 pathway, either through Paquinimod or genetic ablation, improved survival in mice with sepsis by reducing platelet pyroptosis [31]. Another study found that S100A8/A9 exacerbated sepsis-induced lung injury, partly through the P38/STAT3/ERK pathways. Deficiency of S100A8/A9 alleviated pulmonary vascular permeability in CLP mice [32]. In addition, S100A8/A9 participated in sepsis-induced cardiomyopathy via the TLR4-ERK1/2-Drp1 pathway, leading to mitochondrial fission and dysfunction [33]. While we cannot rule out the contribution of other inflammatory mediators, our study provided a fresh perspective on sepsis-induced lung injury by investigating the role of EV S100A8/A9.

Our results indicate that S100A8/A9 may be crucial in promoting the transfer of septic shock-derived EVs to alveolar macrophages. Chakraborty et al. reported that S100A8/A9 was present on the surface of cell membranes and secreted via EVs [34]. Bhardwaj et al. found that cell surface expression of S100A8/A9 in monocytes/macrophages was elevated in acute inflammation, but not in chronic inflammation [35]. It is well recognized that functional membrane proteins can be expressed on the surface of EVs [36]. Therefore, it is highly plausible that septic shock EVs express S100A8/A9 on their surface. Other studies have shown that EVs are internalized via receptor-mediated endocytosis [37]. Pham et al. documented that endocytosis of red blood cell-derived EVs by macrophages triggered the release of cytoplasmic heme, thereby preventing the formation of foam cells in atherosclerosis [38]. Thus, we propose that S100A8/A9 on the surface of septic shock EVs may interact with RAGE and/or TLR4 on alveolar macrophages, prompting the uptake of EVs and initiating an inflammatory response.

It is generally accepted that S100A8/A9 exerts its effect via RAGE and/or TLR4 pathway. Guo et al. revealed that SARS-CoV-2 infection upregulated S100A8 expression, triggering aberrant neutrophil activation via the S100A8/

(See figure on next page.)

**Fig. 7** Transfer of S100A8/A9 from septic EVs to alveolar macrophages. **A** Vybrant DiD-labeled septic shock EVs (100  $\mu$ g/50  $\mu$ l) were administered to C57BL/6 mice (6–8 weeks old) intratracheally. BAL specimens were harvested at 24 h after treatment and examined for F4/80 + DiD + macrophages via flow cytometry. **B** Vybrant DiD-labeled septic shock EVs (red) (100  $\mu$ g/50  $\mu$ l) were administered to C57BL/6 mice (6–8 weeks old) intratracheally. Lung samples were harvested at 24 h and processed for immunostaining with the macrophage marker F4/80 (green), followed by counterstaining with DAPI to visualize cell nuclei. The specimens were then imaged using confocal microscopy. Pulmonary macrophages exhibiting both red and green fluorescence were identified as those that had successfully internalized septic shock EVs. **C** Control or septic shock EVs (100  $\mu$ g/50  $\mu$ l) were administered to C57BL/6 mice (6–8 weeks old) intratracheally. BAL specimens were harvested at 24 h after treatment. Alveolar macrophages were separated and examined for the expression of S100A8/A9. **D** Septic shock EVs (100  $\mu$ g/50  $\mu$ l) were incubated overnight at 4  $^{\circ}$ C with or without an anti-S100A8/A9 neutralization antibody at 100  $\mu$ g/ml and administered to C57BL/6 mice (6–8 weeks old) intratracheally. BAL specimens were harvested at 24 h after treatment. Alveolar macrophages were separated and examined for the expression of S100A8/A9 by Western blot. Data are expressed as mean  $\pm$  SD, n = 8 (**C**), n = 3 (**D**). \*p < 0.05, \*\*p < 0.01

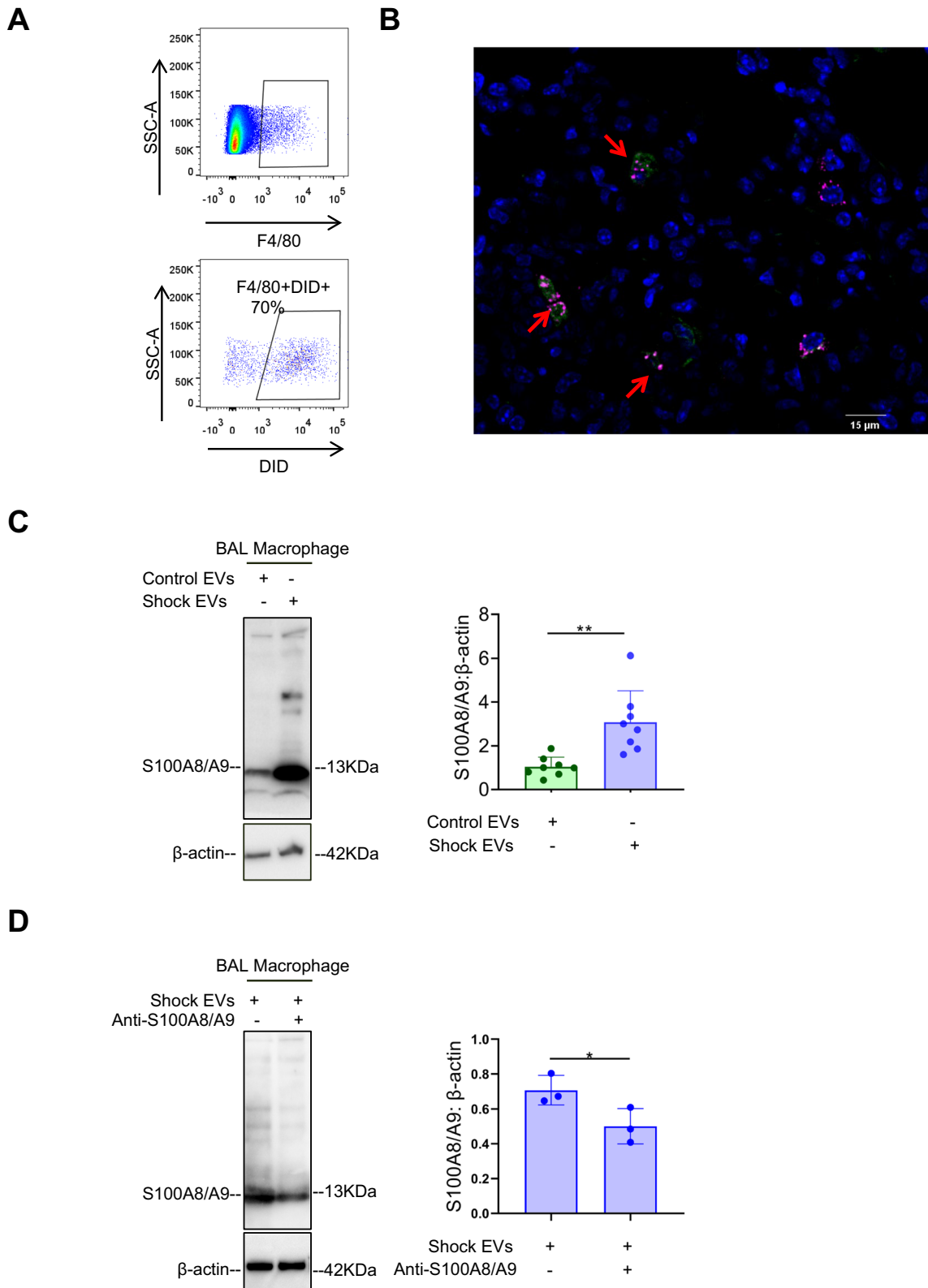


**Fig. 7** (See legend on previous page.)

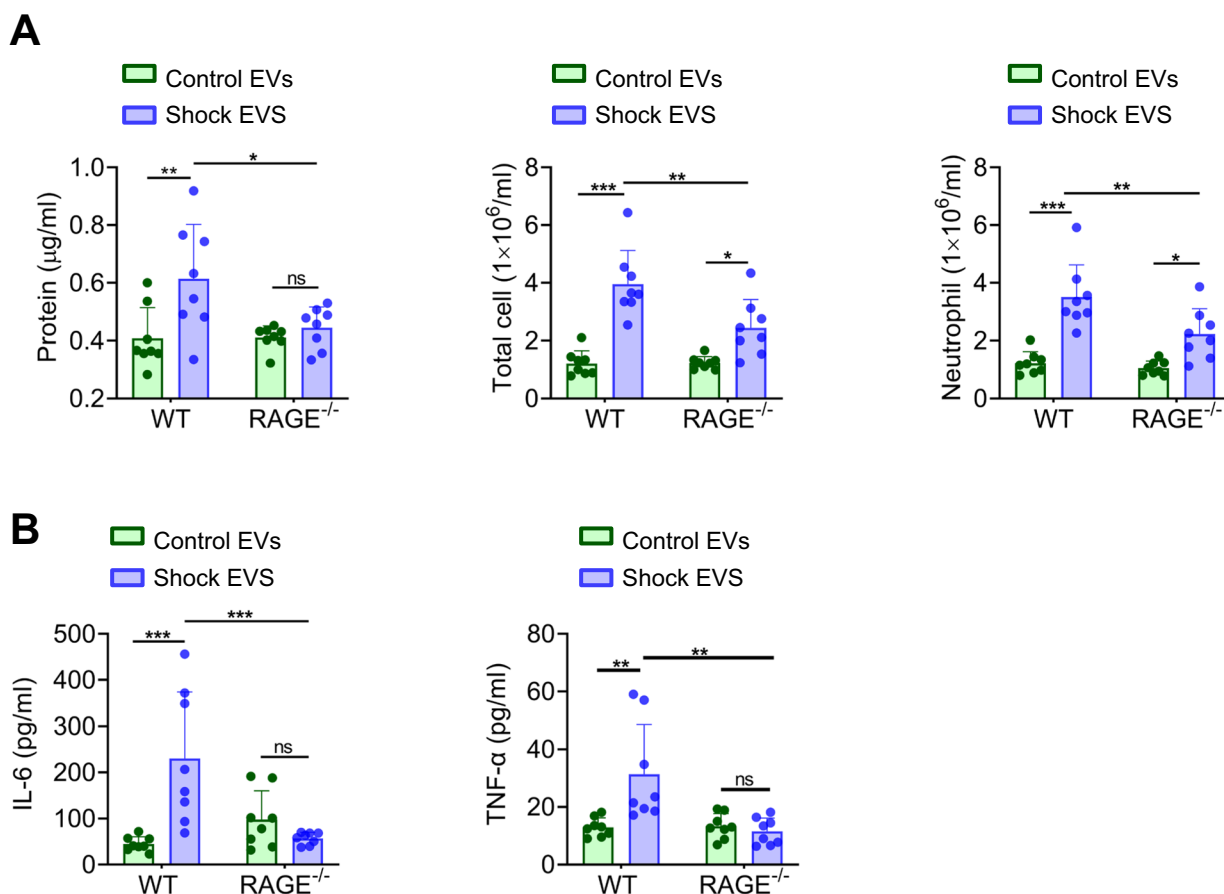


**Fig. 8** Role of RAGE in sepsis EV-evoked acute lung injury. Control or septic shock EVs (100  $\mu\text{g}/50 \mu\text{l}$ ) were injected into RAGE<sup>-/-</sup> or WT C57BL/6 mice intratracheally. Mice were sacrificed 24 h after treatment. **A** BAL was examined for lung injury parameters, which included total protein content, total cell count, and neutrophil count. **B** Levels of BAL IL-6 and TNF- $\alpha$  levels were examined via ELISA. Data are expressed as mean  $\pm$  SD,  $n=8$ . \* $p < 0.05$ , \*\* $p < 0.01$ , \*\*\* $p < 0.001$ . ns: not significant

A9-TLR4 pathway [39]. Our results indicate that septic shock-derived EVs induce lung injury, partly through the S100A8/A9-RAGE pathway. Boyd et al. found that S100A8/A9 contributed to endotoxin-induced cardiomyocyte dysfunction by interacting with RAGE [40]. In peripheral blood mononuclear cells from patients with septic shock, Hofer et al. found that the expression of membrane RAGE was significantly elevated compared to healthy controls. This increase in RAGE expression was accompanied by a marked rise in soluble RAGE (sRAGE) levels in plasma, which is likely attributed to the elevated shedding of membrane RAGE [41]. Consistent with these findings, our results also showed that sRAGE expression in the plasma of septic shock patients was significantly higher than in sepsis patients and healthy controls (Supplemental Fig. 3). However, Chen et al. demonstrated that S100A9 induced macrophage infiltration and cytokine release in the lungs, independently of RAGE or TLR4 signaling [42]. Additionally, Ghavami et al. reported

that S100A8/A9 triggered apoptosis by promoting mitochondrial dysfunction and reducing the expression of anti-apoptotic proteins Bcl-2 and Bcl-xL, independent of RAGE [43].

This study examined the changes in EV S100A8/A9 during septic shock and explored its contribution to acute lung injury. The involvement of EV S100A8/A9 has been documented in the pathogenesis of other diseases. For instance, Saenz-Pipaon et al. revealed that levels of S100A8/A9 in circulating EVs were elevated in patients with peripheral arterial disease and correlated with high amputation risk [44]. Li et al. documented that plasma EVs from systemic sclerosis patients blocked the proliferation and migration of endothelial cells. S100A8/A9 may play an essential role in the process [45]. Burke et al. discovered that chemotactic S100A8/A9 was abundant in EVs generated from myeloid-derived suppressor cells, which are commonly present in cancer patients [46]. Maus et al. demonstrated that human melanoma-derived

EVs altered dendritic cell maturation via S100A8/A9 cargo [47]. However, Joshi et al. found that neutrophil-derived S100A8/A9 modulated platelet activity during acute myocardial infarction via free heterodimer, rather than EVs [48].

In the present report, the results showed that alveolar macrophages were the target cells of sepsis EVs. Macrophages, originating from different sources, have been widely studied as a recipient of EVs. EVs derived from RAW264.7 macrophages pre-treated with LPS enhanced the secretion of IL-6 and TNF- $\alpha$  in naive RAW264.7 cells [28]. LPS-exposed murine BMDMs produced histone-containing EVs which interacted with TLR4, inducing inflammatory response in untreated BMDMs [49]. Endothelial EVs carrying heat shock protein A12B were internalized by RAW264.7 macrophages. EV treatment elevated IL-10 production and decreased TNF- $\alpha$  and IL-1 $\beta$  levels in LPS-stimulated macrophages [50]. Moreover, mycobacteria-infected RAW264.7 macrophages heightened production of EVs containing heat shock protein 70 on the surface. These vesicles induced NF- $\kappa$ B activation and TNF- $\alpha$  secretion in uninfected macrophages [51].

The pathogenic characteristics of sepsis-induced lung injury include activation (M1 polarization) of alveolar macrophages, elevation of proinflammatory cytokines, and infiltration of neutrophils [52]. The current study showed that septic shock EVs induced M1 polarization of macrophages in vitro and in vivo. It is known that M1 macrophages are active producers of proinflammatory cytokines and inducers of neutrophil recruitment [53]. Polarized macrophages could also be parental cells for proinflammatory EVs, resulting in lung injury. Soni et al. showed that intratracheal administration of EVs from LPS-primed alveolar macrophages elevated BAL neutrophil infiltration, protein leakage, and ICAM-1 expression in mice [54]. In an animal model of LPS-evoked lung inflammation, alveolar macrophages were the major contributors for the proinflammatory cytokines in the BAL EVs [55].

There are several limitations in the design of the present study. First, we did not assess the potential of the S100A8/A9 neutralizing antibody to block the effects of septic shock EVs in vivo. Secondly, the study encompassed a sepsis cohort and a septic shock cohort, each with diverse etiologies such as pneumonia, intra-abdominal infection, urinary tract infection, and others. It is unknown whether the origin of the infection modulates the functions of EVs. Thirdly, this study included 28 sepsis patients and 26 septic shock patients. A larger sample size is crucial to validate the potential of EV S100A8/A9 in distinguishing septic shock from sepsis and predicting the onset of ARDS.

## Conclusions

Our study reveals that EV S100A8/A9 holds promise as both a diagnostic marker to differentiate septic shock from sepsis and a prognostic indicator for the onset of ARDS. S100A8/A9-RAGE pathway is at least partially responsible for septic shock EVs-induced acute lung injury. S100A8/A9 may emerge as an appealing therapeutic target for treating sepsis-associated acute lung injury.

## Abbreviations

ARDS	Acute respiratory distress syndrome
EVs	Extracellular vesicles
SOFA	Sequential organ failure assessment
APACHE	Acute physiology and chronic health evaluation
CRP	C-reactive protein
PCT	procalcitonin
ICU	Intensive care unit
PMB	Polymyxin B
RAGE	Receptor for advanced glycation endproducts
CLP	Cecal ligation and puncture
BMDMs	Bone marrow-derived macrophages
BAL	Bronchoalveolar lavage
LPS	Lipopolysaccharide
SD	Standard deviation of the mean
ANOVA	Analysis of variance

## Supplementary Information

The online version contains supplementary material available at <https://doi.org/10.1186/s12931-025-03181-1>.

Supplementary material 1.

Supplementary material 2.

## Acknowledgements

The authors thank the medical and nursing staff at the ICU department of the First Affiliated Hospital of Zhejiang University School of Medicine.

## Author contributions

Conception and design: JW, WW, QS, JXu; Acquisition of Data: JW, WW, TW, GZ, GQ, HQ, RZhang, JXia, YH, RH, RZang, ZL, QS, JXu; Analysis and interpretation: JW, WW, TW, GZ, GQ, HQ, RZhang, JXia, YH, RH, RZang, ZL, QS, JXu. All authors contributed to drafting the manuscript of important intellectual content and final approval of the manuscript.

## Funding

This work was supported by the Basic Public Welfare Research Program of Zhejiang Province (Grant No. LGF22H150010 and LY24H010001), the National Natural Science Foundation of China (Grant No. 82070074, 82272191, and 82370080), the Health Commission of Zhejiang Province (Grant No. 2024KY491), and the Health Commission of Shaoxing (Grant No. 2023SKY100 and 2023SKY103).

## Availability of data and materials

No datasets were generated or analysed during the current study.

## Declarations

### Ethics approval and consent to participate

The study protocol was approved by the ethics committee of the First Affiliated Hospital of Zhejiang University School of Medicine and conducted according to the provisions detailed in Declaration of Helsinki. Written informed consent was obtained from all patients or their legal representative.

Animal study protocol was approved by Institutional Animal Care and Use Committee of Zhejiang University School of Medicine.

#### Consent for publication

Not applicable.

#### Competing interests

The authors declare no competing interests.

#### Author details

<sup>1</sup>The Children's Hospital of Zhejiang University School of Medicine and National Clinical Research Center for Child Health, 3333 Binsheng Road, Hangzhou 310052, Zhejiang, China. <sup>2</sup>The First Affiliated Hospital of Zhejiang University School of Medicine, 79 Qingchun Road, Hangzhou 310006, Zhejiang, China. <sup>3</sup>Shaoxing Second Hospital, 123 Yanan Road, Shaoxing 312000, Zhejiang, China. <sup>4</sup>Department of Thoracic and Cardiovascular Surgery, The Children's Hospital of Zhejiang University School of Medicine, 3333 Binsheng Road, Hangzhou 310052, Zhejiang, China.

Received: 11 November 2024 Accepted: 5 March 2025

Published online: 18 March 2025

#### References

- McNicholas BA, Rooney GM, Laffey JG. Lessons to learn from epidemiologic studies in ARDS. *Curr Opin Crit Care*. 2018;24(1):41–8.
- Laffey JG, Matthay MA. Fifty years of research in ARDS. Cell-based therapy for acute respiratory distress syndrome. Biology and potential therapeutic value. *Am J Respir Crit Care Med*. 2017;196(3):266–73.
- Bellani G, Laffey JG, Pham T, Fan E, Brochard L, Esteban A, Gattinoni L, van Haren F, Larsson A, McAuley DF, et al. Epidemiology, patterns of care, and mortality for patients with acute respiratory distress syndrome in intensive care units in 50 countries. *JAMA*. 2016;315(8):788–800.
- Singer M, Deutschman CS, Seymour CW, Shankar-Hari M, Annane D, Bauer M, Bellomo R, Bernard GR, Chiche JD, Cooper-Smith CM, et al. The third international consensus definitions for sepsis and septic shock (Sepsis-3). *JAMA*. 2016;315(8):801–10.
- Rudd KE, Johnson SC, Agesa KM, Shackelford KA, Tsoi D, Kievlan DR, Colombara DV, Ikuta KS, Kisssoon N, Finfer S, et al. Global, regional, and national sepsis incidence and mortality, 1990–2017: analysis for the Global Burden of Disease Study. *Lancet*. 2020;395(10219):200–11.
- Thery C, Witwer KW, Aikawa E, Alcaraz MJ, Anderson JD, Andriantsitohaina R, Antoniou A, Arab T, Archer F, Atkin-Smith GK, et al. Minimal information for studies of extracellular vesicles 2018 (MISEV2018): a position statement of the International Society for Extracellular Vesicles and update of the MISEV2014 guidelines. *J Extracell Vesicles*. 2018;7(1):1535750.
- Chargaff E, West R. The biological significance of the thromboplastic protein of blood. *J Biol Chem*. 1946;166(1):189–97.
- Wolf P. The nature and significance of platelet products in human plasma. *Br J Haematol*. 1967;13(3):269–88.
- Pan BT, Johnstone RM. Fate of the transferrin receptor during maturation of sheep reticulocytes in vitro: selective externalization of the receptor. *Cell*. 1983;33(3):967–78.
- Yanez-Mo M, Siljander PR, Andreu Z, Zavec AB, Borrás FE, Buzas EI, Buzas K, Casal E, Cappello F, Carvalho J, et al. Biological properties of extracellular vesicles and their physiological functions. *J Extracell Vesicles*. 2015;4:27066.
- Zhang Y, Liu Y, Liu H, Tang WH. Exosomes: biogenesis, biologic function and clinical potential. *Cell Biosci*. 2019;9:19.
- Qiu G, Zheng G, Ge M, Wang J, Huang R, Shu Q, Xu J. Mesenchymal stem cell-derived extracellular vesicles affect disease outcomes via transfer of microRNAs. *Stem Cell Res Ther*. 2018;9(1):320.
- Wang J, Huang R, Xu Q, Zheng G, Qiu G, Ge M, Shu Q, Xu J. Mesenchymal stem cell-derived extracellular vesicles alleviate acute lung injury via transfer of miR-27a-3p. *Crit Care Med*. 2020;48(7):e599–610.
- Mastrorandi ML, Mostefai HA, Meziari F, Martinez MC, Asfar P, Andriantsitohaina R. Circulating microparticles from septic shock patients exert differential tissue expression of enzymes related to inflammation and oxidative stress. *Crit Care Med*. 2011;39(7):1739–48.
- Li G, Wang B, Ding X, Zhang X, Tang J, Lin H. Plasma extracellular vesicle delivery of miR-210-3p by targeting ATG7 to promote sepsis-induced acute lung injury by regulating autophagy and activating inflammation. *Exp Mol Med*. 2021;53(7):1180–91.
- Xu J, Feng Y, Jeyaram A, Jay SM, Zou L, Chao W. Circulating plasma extracellular vesicles from septic mice induce inflammation via microRNA- and TLR7-dependent mechanisms. *J Immunol*. 2018;201(11):3392–400.
- Edgeworth J, Gorman M, Bennett R, Freemont P, Hogg N. Identification of p8,14 as a highly abundant heterodimeric calcium binding protein complex of myeloid cells. *J Biol Chem*. 1991;266(12):7706–13.
- Ryckman C, Vandal K, Rouleau P, Talbot M, Tessier PA. Proinflammatory activities of S100: proteins S100A8, S100A9, and S100A8/A9 induce neutrophil chemotaxis and adhesion. *J Immunol*. 2003;170(6):3233–42.
- Skronska-Wasek W, Durlanik S, Le HQ, Schroeder V, Kitt K, Garnett JP, Pflanz S. The antimicrobial peptide S100A8/A9 produced by airway epithelium functions as a potent and direct regulator of macrophage phenotype and function. *Eur Respir J*. 2022;59(4):2002732.
- Dubois C, Marce D, Faivre V, Lukaszewicz AC, Junot C, Fenaille F, Simon S, Becher F, Morel N, Payen D. High plasma level of S100A8/S100A9 and S100A12 at admission indicates a higher risk of death in septic shock patients. *Sci Rep*. 2019;9(1):15660.
- Qiu G, Fan J, Zheng G, He J, Lin F, Ge M, Huang L, Wang J, Xia J, Huang R, et al. Diagnostic potential of plasma extracellular vesicle miR-483-3p and Let-7d-3p for sepsis. *Front Mol Biosci*. 2022;9:814240.
- Sun C, Xie Y, Zhu C, Guo L, Wei J, Xu B, Song Y, Qin H, Li X. Serum Mrp 8/14 as a potential biomarker for predicting the occurrence of acute respiratory distress syndrome induced by sepsis: a retrospective controlled study. *J Inflamm Res*. 2024;17:2939–49.
- Kuipers MT, Vogl T, Aslami H, Jongsma G, van den Berg E, Vlaar AP, Roelofs JJ, Juffermans NP, Schultz MJ, van der Poll T, et al. High levels of S100A8/A9 proteins aggravate ventilator-induced lung injury via TLR4 signaling. *PLoS ONE*. 2013;8(7):e68694.
- Griffiths MJ, McAuley DF. RAGE: a biomarker for acute lung injury. *Thorax*. 2008;63(12):1034–6.
- Azevedo LC, Janiszewski M, Pontieri V, Pedro Mde A, Bassi E, Tucci PJ, Laurindo FR. Platelet-derived exosomes from septic shock patients induce myocardial dysfunction. *Crit Care*. 2007;11(6):R120.
- Mortaza S, Martinez MC, Baron-Menguy C, Burban M, de la Bourdonnaye M, Fizanne L, Pierrot M, Cales P, Henrion D, Andriantsitohaina R, et al. Detrimental hemodynamic and inflammatory effects of microparticles originating from septic rats. *Crit Care Med*. 2009;37(6):2045–50.
- Boisrame-Helms J, Delabranche X, Degirmenci SE, Zobairi F, Berger A, Meyer G, Burban M, Mostefai HA, Levy B, Toti F, et al. Pharmacological modulation of procoagulant microparticles improves haemodynamic dysfunction during septic shock in rats. *Thromb Haemost*. 2014;111(1):154–64.
- Essandoh K, Yang L, Wang X, Huang W, Qin D, Hao J, Wang Y, Zingarelli B, Peng T, Fan GC. Blockade of exosome generation with GW4869 dampens the sepsis-induced inflammation and cardiac dysfunction. *Biochim Biophys Acta*. 2015;1852(11):2362–71.
- Wang Y, Shi Y, Shao Y, Lu X, Zhang H, Miao C. S100A8/A9(hi) neutrophils induce mitochondrial dysfunction and PANoptosis in endothelial cells via mitochondrial complex I deficiency during sepsis. *Cell Death Dis*. 2024;15(6):462.
- Jakobsson G, Papareddy P, Andersson H, Mulholland M, Bhongir R, Ljungcrantz I, Engelbertsen D, Bjorkbacka H, Nilsson J, Manea A, et al. Therapeutic S100A8/A9 blockade inhibits myocardial and systemic inflammation and mitigates sepsis-induced myocardial dysfunction. *Crit Care*. 2023;27(1):374.
- Su M, Chen C, Li S, Li M, Zeng Z, Zhang Y, Xia L, Li X, Zheng D, Lin Q, et al. Gasdermin D-dependent platelet pyroptosis exacerbates NET formation and inflammation in severe sepsis. *Nat Cardiovasc Res*. 2022;1(8):732–47.
- Yu J, Zhao B, Pi Q, Zhou G, Cheng Z, Qu C, Wang X, Kong L, Luo S, Du D, et al. Deficiency of S100A8/A9 attenuates pulmonary microvascular leakage in septic mice. *Respir Res*. 2023;24(1):288.
- Wu F, Zhang YT, Teng F, Li HH, Guo SB. S100a8/a9 contributes to sepsis-induced cardiomyopathy by activating ERK1/2-Drp1-mediated mitochondrial fission and respiratory dysfunction. *Int Immunopharmacol*. 2023;115:109716.

34. Chakraborty P, Bjork P, Kallberg E, Olsson A, Riva M, Morgelin M, Liberg D, Ivars F, Leanderson T. Vesicular location and transport of S100A8 and S100A9 proteins in monocytoïd cells. *PLoS ONE*. 2015;10(12):e0145217.
35. Bhardwaj RS, Zotz C, Zwadlo-Klarwasser G, Roth J, Goebeler M, Mahnke K, Falk M, Meinardus-Hager G, Sorg C. The calcium-binding proteins MRP8 and MRP14 form a membrane-associated heterodimer in a subset of monocytes/macrophages present in acute but absent in chronic inflammatory lesions. *Eur J Immunol*. 1992;22(7):1891–7.
36. Yang Y, Hong Y, Cho E, Kim GB, Kim IS. Extracellular vesicles as a platform for membrane-associated therapeutic protein delivery. *J Extracell Vesicles*. 2018;7(1):1440131.
37. Teng F, Fussenegeger M. Shedding light on extracellular vesicle biogenesis and bioengineering. *Adv Sci (Weinh)*. 2020;8(1):2003505.
38. Pham TT, Le AH, Dang CP, Chong SY, Do DV, Peng B, Jayasinghe MK, Ong HB, Hoang DV, Louise RA, et al. Endocytosis of red blood cell extracellular vesicles by macrophages leads to cytoplasmic heme release and prevents foam cell formation in atherosclerosis. *J Extracell Vesicles*. 2023;12(8):e12354.
39. Guo Q, Zhao Y, Li J, Liu J, Yang X, Guo X, Kuang M, Xia H, Zhang Z, Cao L, et al. Induction of alarmin S100A8/A9 mediates activation of aberrant neutrophils in the pathogenesis of COVID-19. *Cell Host Microb*. 2021;29(2):222–35.
40. Boyd JH, Kan B, Roberts H, Wang Y, Walley KR. S100A8 and S100A9 mediate endotoxin-induced cardiomyocyte dysfunction via the receptor for advanced glycation end products. *Circ Res*. 2008;102(10):1239–46.
41. Hofer S, Uhle F, Fleming T, Hell C, Schmoch T, Bruckner T, Weigand MA, Brenner T. RAGE-mediated inflammation in patients with septic shock. *J Surg Res*. 2016;202(2):315–27.
42. Chen B, Miller AL, Rebelatto M, Brewah Y, Rowe DC, Clarke L, Czapiga M, Rosenthal K, Imamichi T, Chen Y, et al. S100A9 induced inflammatory responses are mediated by distinct damage associated molecular patterns (DAMP) receptors in vitro and in vivo. *PLoS ONE*. 2015;10(2):e0115828.
43. Ghavami S, Kerkhoff C, Chazin WJ, Kadkhoda K, Xiao W, Zuse A, Hashemi M, Eshraghi M, Schulze-Osthoff K, Klönisch T, et al. S100A8/9 induces cell death via a novel, RAGE-independent pathway that involves selective release of Smac/DIABLO and Omi/HtrA2. *Biochim Biophys Acta*. 2008;1783(2):297–311.
44. Saenz-Pipaon G, San Martín P, Planell N, Maïllo A, Ravassa S, Vilas-Zornoza A, Martínez-Aguilar E, Rodríguez JA, Alameda D, Lara-Astiaso D, et al. Functional and transcriptomic analysis of extracellular vesicles identifies calprotectin as a new prognostic marker in peripheral arterial disease (PAD). *J Extracell Vesicles*. 2020;9(1):1729646.
45. Li L, Zuo X, Xiao Y, Liu D, Luo H, Zhu H. Neutrophil-derived exosome from systemic sclerosis inhibits the proliferation and migration of endothelial cells. *Biochem Biophys Res Commun*. 2020;526(2):334–40.
46. Burke M, Choksawangkar W, Edwards N, Ostrand-Rosenberg S, Fenselau C. Exosomes from myeloid-derived suppressor cells carry biologically active proteins. *J Proteome Res*. 2014;13(2):836–43.
47. Maus RLG, Jakub JW, Nevala WK, Christensen TA, Noble-Orcutt K, Sachs Z, Hieken TJ, Markovic SN. Human melanoma-derived extracellular vesicles regulate dendritic cell maturation. *Front Immunol*. 2017;8:358.
48. Joshi A, Schmidt LE, Burnap SA, Lu R, Chan MV, Armstrong PC, Baig F, Gutmann C, Willeit P, Santer P, et al. Neutrophil-derived protein S100A8/A9 alters the platelet proteome in acute myocardial infarction and is associated with changes in platelet reactivity. *Arterioscler Thromb Vasc Biol*. 2022;42(1):49–62.
49. Nair RR, Mazza D, Brambilla F, Gorzanelli A, Agresti A, Bianchi ME. LPS-challenged macrophages release microvesicles coated with histones. *Front Immunol*. 2018;9:1463.
50. Tu F, Wang X, Zhang X, Ha T, Wang Y, Fan M, Yang K, Gill PS, Ozment TR, Dai Y, et al. Novel role of endothelial derived exosomal HSPA12B in regulating macrophage inflammatory responses in polymicrobial sepsis. *Front Immunol*. 2020;11:825.
51. Anand PK, Anand E, Bleck CK, Anes E, Griffiths G. Exosomal Hsp70 induces a pro-inflammatory response to foreign particles including mycobacteria. *PLoS ONE*. 2010;5(4):e10136.
52. Su X, Matthey MA, Malik AB. Requisite role of the cholinergic alpha7 nicotinic acetylcholine receptor pathway in suppressing Gram-negative sepsis-induced acute lung inflammatory injury. *J Immunol*. 2010;184(1):401–10.
53. Murray PJ. Macrophage polarization. *Annu Rev Physiol*. 2017;79:541–66.
54. Soni S, Wilson MR, O’Dea KP, Yoshida M, Katbeh U, Woods SJ, Takata M. Alveolar macrophage-derived microvesicles mediate acute lung injury. *Thorax*. 2016;71(11):1020–9.
55. Ye C, Li H, Bao M, Zhuo R, Jiang G, Wang W. Alveolar macrophage-derived exosomes modulate severity and outcome of acute lung injury. *Aging (Albany NY)*. 2020;12(7):6120–8.

## Publisher’s Note

Springer Nature remains neutral with regard to jurisdictional claims in published maps and institutional affiliations.